2014 IEEE International Conference on Robotics & Automation (ICRA)
Hong Kong Convention and Exhibition Center
May 31 - June 7, 2014. Hong Kong, China

Power Efficient Balancing Control for Humanoids based on Approximate Optimal Ankle Compliance Regulation

Mohamad Mosadeghzad, Nikos G. Tsagarakis, Gustavo A. Medrano-Cerda and Darwin G. Caldwell

***Abstract*— The balance control of humanoid robots against external perturbations is a fundamental prerequisite for operating in unstructured environments where physical interaction may unexpectedly occur. These balancing actions can be very demanding in terms of power and torque requirements for ankle joints especially after strong and sudden impacts. In this work, an optimal control problem is formulated for the linearized inverted pendulum model to reduce the peak power requirements during ankle balancing strategy. This optimal control which reduces peak torque and power is computed numerically and approximated by a piecewise linear function of the states called the approximate optimal compliance regulator. The balancing ability of this compliance regulator is evaluated against other optimal compliance methods. The stability of the linearly switching approximated optimal compliance regulator is determined from practical perspective using quadratic stability and parameter dependent Lyapunov functions. The efficacy of the proposed stabilizer is validated for a compliant humanoid.**

I. Introduction

Humanoids will have to demonstrate similar balancing capabilities as humans to cope with unanticipated external disturbances during standing and walking. Although keeping balance is the main concern, proper demanding power is essential for autonomous humanoids and humans.

Ankle, ankle-hip and stepping are well known balancing strategies for humans and humanoids. [1], [2] revealed that, for small and slow disturbances in the sagittal plane, humans sway the center of mass (CoM) as an inverted pendulum mainly about the ankle [3]. This muscle activation pattern has been named ankle strategy. Regulation of impedance during ankle balancing is studied in humans [4].

It has been shown that humans during balancing not only regulate the center of mass but also modulate their joint's impedance by varying their muscle activation while keeping the consumption power inside the capability range of muscles. Many works use the idea of Cartesian impedance regulation for keeping balance of humanoids [5]–[7].

The effect of ankle stiffness on robot's stability has been also studied during walking [8]. In addition, it is explored for improving the energy efficiency during walking [9]. The work in [10] explores the use of passive elastic elements for improving the robot stability and tries to identify suitable range of passive stiffness to achieve this goal.

Mohamad Mosadeghzad, Nikos G. Tsagarakis, Gustavo A. Medrano-Cerda and Darwin G. Caldwell are with the Department of Advanced Robotics, Istituto Italiano di Tecnologia, via Morego 30, 16163 Genova, Italy. Email: (mmzad83.basu@gmail.com, nikos.tsagarakis, gustavo.cerda, darwin.caldwell)@iit.it. Mohamad Mosadeghzad is also with Faculty of Engineering, University of Genoa.

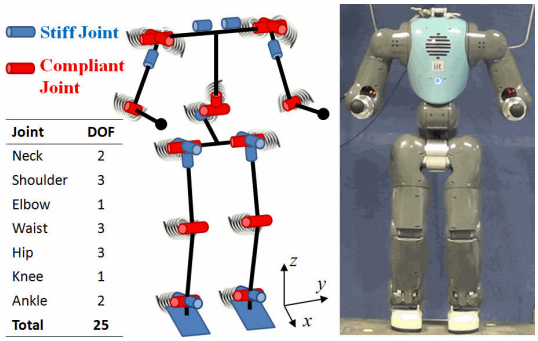

Fig. 1. Full body COMAN and its kinematics model

In most of the above mentioned works the impedance were experimentally adjusted without consideration of the power consumption. In the same path of works [11], [12] which respond to demands of suitable compliance profiles exploiting variable impedance actuation technology [13] for different tasks and performance indexes, this work proposes the use of optimal control to provide an ankle stabilizer which minimizes the power requirements of the balancing effort. In the previous work of the author [14] it is shown how the ankle impedance can be calculated analytically to provide the optimal balancing controller when the robot is subject to impact. This paper is an extension of [14] and contributes with the development of an optimal ankle compliance balancing strategy which targets to reduce the power requirements of the balancing action.

The contribution of this paper is that it permits to derive a low power ankle compliance regulation startegy for the humanoid balancing problem by utilizing optimal control. The accurate low power optimal ankle stabilizer is addressed and the condition of a class of possible approximate feedback controller is presented. A piecewise linear ankle torque model from optimal balancing perspective is proposed which is simple enough to be implemented on humanoids with impedance control capability. Hence, differently from the optimal ankle stabilizer proposed in [14] where ankle compliance is kept constant for a range of impacts, in the proposed method the ankle compliance is regulated to reduce the peake power demand for the ankle motor. The approximate optimal piecewise linear compliance provides whole body balance for higher range of impacts, reducing the ankle torque and power using lower values of damping.

The paper is organized as follows. Section II introduces COMAN humanoid and its model. II-A concisely indicates the constant linear compliant ankle strategy while II-B

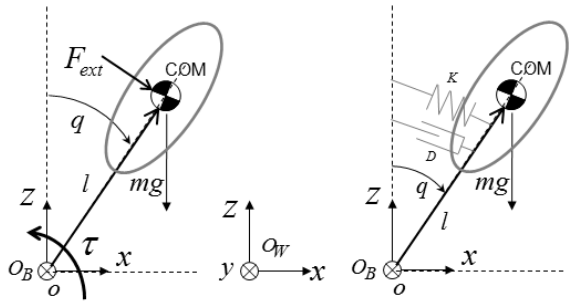

Fig. 2. Inverted Pendulum Model. Left: Free body diagram of the robot in sagittal plane; Right: Ankle torque replaced by compliance.

TABLE I

MODELING PARAMETERS OF THE COMAN HUMANOID LOWER BODY

m:	mass of the lower body; $16.5\ Kg$
I_c:	inertia tensor around the CoM; $\simeq 0.9537\ Kgm^2$
I:	inertia tensor around the ankle pivot; $I = I_c + ml^2$
l:	nominal pendulum length from the CoM to the pivot; $34\ cm$
q:	angular position of the link
K_p:	ankle stiffness constant of passive spring; $400\ \frac{Nm}{rad}$
D_p:	ankle passive damping constant; $\simeq 2.5\ \frac{Nm \cdot s}{rad}$
K, D:	resultant stiffness/damping of the CoM around ankle
d_1:	upper limit of x_{cop} based on the robot foot size; $11.5\ cm$
d_2:	lower limit of x_{cop} based on the robot foot size; $4.5\ cm$
ξ:	damping ratio of the ankle impedance

elaborates a constrained optimal control aimed at reducing the maximum motor power and torque. II-C suggests an approximate optimal low power piecewise linear compliance regulation strategy. The study is concluded in section III.

II. Compliant Ankle Strategy on Humanoids

The **Co**mpliant Hu**Man**oid humanoid COMAN [15]–[17] robot (see Fig. 1) is modeled as an inverted pendulum model [18] with mechanical properties of mass m and moment of inertia I_c around the center of mass (CoM), as shown in Fig. 2. In this figure the origin of the local reference frame O_B is located in the midpoint of right and left foot local reference frames. Pendulum angle (ankle pitch) is represented by q and F_{ext} is the frontal external disturbance (impact or a constant force) exerted to the body's main axis. The dynamic equation of motion is derived as below:

$$-\tau + l \cdot F_{ext} + mglsin(q) = (I_c + ml^2)\ddot{q}. \tag{1}$$

The parameters of the COMAN are summarized in Table I. The center of pressure in the anteroposterior axis for the robot feet (x_{cop}) is given by:

$$x_{cop} = \frac{\tau}{m(g + \ddot{z})}, \tag{2}$$

where $z = lcos(q)$ is the center of mass height. Assuming a range of motion within $-10^\circ < q < 10^\circ$ the height variation is small and therefore the effect of $\ddot{z}$ can be neglected.

A. Optimal Constant Linear Compliance Stabilizer

In the case of an impact, the force in (1) can be eliminated by taking into account an initial CoM velocity $\dot{q_0}$ as a result of the applied impact force. Considering control input, $u = \tau$ and the system states, $x = (q, \dot{q})$, the linearized system (1) around $q = 0$ can be presented as:

$$\begin{cases} \dot{x} & = Ax + Bu, \\ A & = \begin{pmatrix} 0 & 1 \\ \frac{mgl}{I} & 0 \end{pmatrix}, B = \begin{pmatrix} 0 \\ -\frac{1}{I} \end{pmatrix}, \\ x_1(0) & = 0, x_2(0) = \dot{q_0}, \end{cases} \tag{3}$$

where I is the moment of inertia around pivot point.

The x_{cop} inside the convex foot polygon is a sufficient criterion for the whole body dynamic stability of humanoid. Therefore, an optimization cost function will be defined as the minimum deviation of x_{cop} squared. Moreover, one can consider the center of mass projection on the ground as an additional criterion of the static stability. This will result in the introduction of a penalty on the ankle deflection, q. The overall cost function will be:

$$J_1 = \int_0^\infty (x_{cop}^2 + \delta x_{com}^2)\mathrm{d}t = \int_0^\infty (\frac{u^2}{(mg)^2} + \delta l^2 q^2)\,\mathrm{d}t, \tag{4}$$

where δ indicates the weight of the x_{com} deviation. J_1 reduces the problem to a standard Linear Quadratic Regulator (LQR) and leads to a solution of the algebraic Riccati equation and a control input (u) which is linear feedback of states [19]. In order to satisfy the stability of the feedback controller, δ should lie between these limits: $-1 < \delta < \infty$.

In [14] it was shown that minimizing the cost J_1 using Riccati equations yields an optimal feedback given by:

$$\tau_1 = Kq + D\dot{q}, \tag{5}$$

where K and D are the resultant torsional stiffness and damping. The optimal constant compliance is given by:

$$\begin{cases} K = mgl(1 + \sqrt{1+\delta}), \\ D = mg\sqrt{2\frac{I \cdot l(1+\sqrt{1+\delta})}{mg}}, \\ \xi = \frac{\sqrt{(2(1+\sqrt{1+\delta}))}}{2\sqrt{1+\delta}}. \end{cases} \tag{6}$$

where ξ is the damping ratio of the system and can be $0 < \xi < \infty$. In order to ensure asymptotic stability of the robot, K should be $mgl < K$ since $-1 < \delta < \infty$. Stiffness and damping are related as:

$$\frac{D}{I} = 2\xi\omega_n = 2\xi\sqrt{\frac{K - mgl}{I}}. \tag{7}$$

where ω_n is natural frequency of the inverted pendulum. Simulation results for different initial CoM velocities using the optimal stiffness and damping values (6) for $\delta = 0$ or $\xi = 1$ are presented in Fig. 3.

It is clear that the initial jump of x_{cop} as seen in Fig. 3 is because of the torque generated by the damping component. $max(\dot{q_0}) = \frac{mgd_1}{D}$ (see (11)). This is derived from (5) for zero q. Initial velocities larger than $max(\dot{q_0})$ will simply force the x_{cop} to the boundary causing the robot to tip over around the foot edge.

B. Optimal Low Peak Power Stabilizer

In this subsection an optimal control problem is constrained to not only reduce the peak power demand of ankle but also satisfy whole body balance requirement of the humanoid which is to keep x_{cop} inside the support

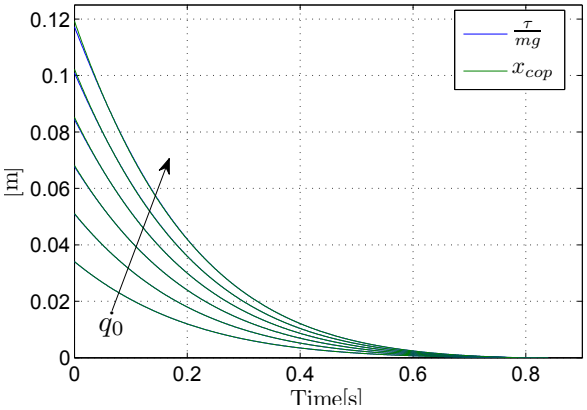

Fig. 3. x_{cop} and τ/mg deviation of robot after impact due to initial velocities from 0.2 to $0.7 rad/sec$ by incremental of $0.1 rad/sec$

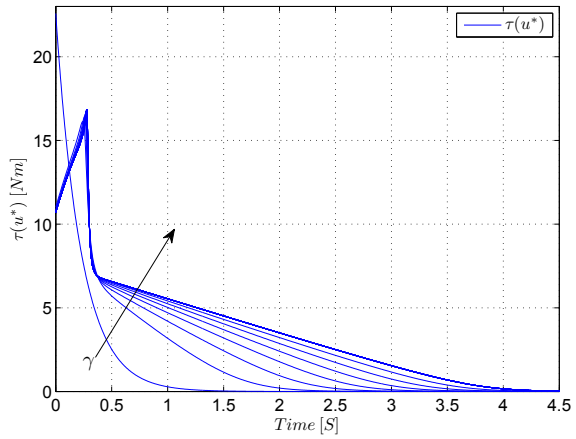

Fig. 4. Optimal control input, u^* due to impact equivalent to initial velocity of 0.9 for γ from zero to 700 by incremental of 100.

polygon during the transient after the impact is applied. Since the maximum velocity and torque of inverted pendulum occur at the instant of an impulsive impact, peak power demand $\dot{q}\tau$ from motor is at this time. In the case of using linear feedback of states (5) the peak power is equal to $D(\dot{q_0})^2$. Therefore reducing peak power can be explained as decreasing the magnitude of the damping feedback gain at the time of the impact. One option is to add a quadratic velocity $(\dot{q})^2$ term to the functional of J_1, (4). The solution can be obtained from the Ricatti equation. However, this increases the magnitude of the damping gain D. A second option is to add a term that is proportional to the power $\dot{q}\tau$ but this term does not affect the gains K and D. The reason is that total mechanical energy, $\int_0^\infty \dot{q}\tau \, \mathrm{d}t = \frac{1}{2} I \dot{q_0}^2$ is constant and cannot be minimized by optimal control. This result can be confirmed by finding Riccati and LQR gains which result in same compliance as (6).

Reducing peak power demand can be introduced by adding the term $(\dot{q}\tau)^2$ in (4). This term is divided by $(mg)^2$ to be scaled in a close range of x_{cop}. The performance cost to be minimized is therefore:

$$J_2 = \int_0^\infty (x_{cop}^2 + \delta x_{com}^2 + \frac{\gamma}{(mg)^2}(\dot{q}\tau)^2)\mathrm{d}t, \qquad (8)$$

where γ is a positive scalar constant weight. Zero value of γ means power is not considered at all and infinity means that only power matters and x_{cop} could be even infinite which means no body balancing can be reached for humanoid. The difficulty is that (8) is not an LQR problem. However still similar to all optimal control problems the objective is minimizing the Hamiltonian function which can be constructed as follow:

$$\mathcal{H} = \frac{u^2}{(mg)^2} + \delta l^2 x_1^2 + \frac{\gamma}{(mg)^2}(x_2 u)^2 + \lambda_1 \dot{x_1} + \lambda_2 \dot{x_2}, \quad (9)$$

where λ_1, λ_2 are costate variables. To minimize $\mathcal{H}$ for a boundary value problem it is enough to solve:

$$\begin{cases} \dot{x}_1 = x_2, \\ \dot{x}_2 = \frac{mglx_1}{I} - \frac{u}{I} + \frac{l \cdot F_{ext}}{I}, \\ \frac{\partial \mathcal{H}}{\partial x_1} = -\dot{\lambda}_1 = 2\delta l^2 x_1 + \lambda_2 \frac{mgl}{I}, \\ \frac{\partial \mathcal{H}}{\partial x_2} = -\dot{\lambda}_2 = \frac{2\gamma x_2 u^2}{(mg)^2} + \lambda_1. \end{cases} \qquad (10)$$

The initial condition for solving these system of differential equations are $x_1(0) = 0, x_2(0) = \dot{q_0}, x_1(\infty) = 0, x_2(\infty) = 0$.

So far, for small impacts, no limits are placed on the control input and states since x_{cop} stays inside the feet polygon. However, this is not the case for large impact forces. Considering the foot size and boundary positions d_1 and $-d_2$ and the fact that x_{cop} should be always inside the foot polygon the following limits for the ankle torque can be derived $-d_2 < \frac{\tau}{mg} < d_1$ or $-mgd_2 < u < mgd_1$. According to minimum Pontryagin principle [19], the optimal input u^*, regardless of the optimization cost function (J_1 or J_2) and any values of δ and γ, is:

$$\begin{cases} u^* = mgd_1 & u > mgd_1, \\ u^* = u & -mgd_2 < u < mgd_1, \\ u^* = -mgd_2 & u < -mgd_2. \end{cases} \qquad (11)$$

Equations (10) and (12) should be solved numerically as a set of simultaneous differential and algebraic equations to compute optimal control input, u^* while the input is not saturated otherwise (11) should be considered.

$$\frac{\partial \mathcal{H}}{\partial u} = 0 \rightarrow u^* = \frac{\lambda_2 (mg)^2}{I(2+2\gamma x_2^2)}. \qquad (12)$$

Setting $\delta = 0$ and using different initial velocities, $\dot{q_0} = \pm\{0.5,\ 0.8,\ 0.9\}$, (10) and (12) were solved in MATLAB using the boundary value problem solver *bvp5c*. Several values for γ were chosen varying from 0 to 700. Fig. 4 to Fig. 7 show the relevant results for $\dot{q_0} = 0.9\ rad/sec$. Fig. 7 shows power consumption of the ankle. It is clear from this plot that adding the $(\dot{q}\tau)^2$ term to the functional can reduce the peak power of ankle around fifty percent and similarly decreases the damping approximately by 50% (in comparison with $\gamma = 0$).

From Fig. 4 it is evident that the optimal torque at the initial time has a significant reduction in peak values for non zero γ. The peak reduction in torque directly affects the x_{cop}, (2) and reduces the likelihood of the x_{cop} leaving the support polygon. This improves the whole body balance stability for high level of impacts. From Fig. 5 it is clear that by increasing γ settling time and maximum x_{com} deviation will rise.

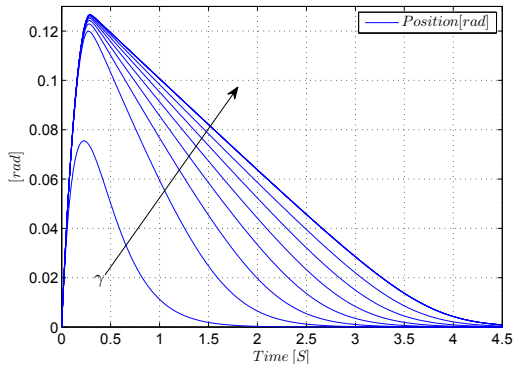

Fig. 5. Position, $q[rad]$ due to impact equivalent to initial velocity of 0.9 for γ from zero to 700 by incremental of 100 with optimal controller (12) .

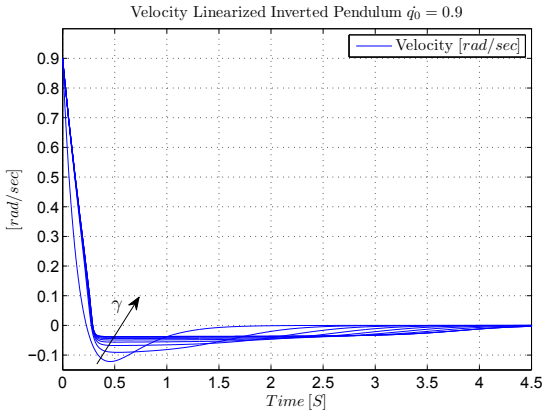

Fig. 6. Velocity, $\dot{q}[rad/s]$ due to impact equivalent to initial velocity of 0.9 for γ from zero to 700 by incremental of 100 with optimal controller (12).

C. Approximate Optimal Compliance Regulator: Peak Power Reduction

For nonzero γ, the cost function (8) gives an optimal control law that cannot be expressed as a linear feedback of the states (5). It is desired to have a feedback controller rather than a feed forward open loop controller as Fig. 4. A feedback controller is more robust to uncertainties of the modeling and disturbances. Also feedback controllers are more convenient in practical implementations. Therefore, in this section the target will be finding an approximate function $u = f(x_1, x_2)$ for u^*. This function could be potentially

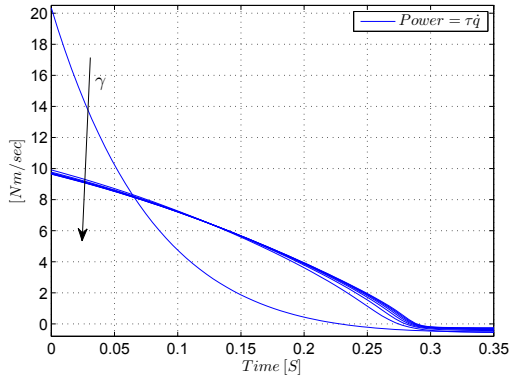

Fig. 7. Instantaneous power due to an impulsive impact equivalent to initial velocity of 0.9 for γ from zero to 700 by incremental of 100 with optimal controller (12).

nonlinear. Also it must result in a globally asymptotically stable closed loop system with equilibrium at zero.

In general, the second order system of the form $\ddot{q}+b(\dot{q})+c(q)=0$, where b and c are continuous functions verifying the sign conditions:

$$\begin{cases} \dot{q}b(\dot{q}) > 0, \text{ for } & \dot{q} \neq 0, \\ qc(q) > 0, \text{ for } & q \neq 0, \end{cases} \tag{13}$$

cannot be stabilized at an equilibrium value other than the origin. Then the origin is globally asymptotically stable [20].

The desired model $f(.)$ should have a minimum set of parameters, physical meaning and be easy enough to be implemented on a real platform. Finding such a nonlinear function of states for humanoid ankle balancing strategy is not trivial.

For providing better fit than linear model a piecewise linear model is considered in the subsequent analysis. As it can be noticed from Fig. 4 the behavior of optimal control signal changes significantly by introducing a small value of γ. Fig. 4 to Fig. 7 imply that the trend of control has two different regimes. The first is from zero to maximum x_{com} deviation where the velocity of CoM is near zero and the second is when the inverted pendulum is going back to its initial position. By increasing γ these two trends can be distinguished easier and the significant reduction of the control signal is more significant. This suggests the following function to approximate the optimal control:

$$\begin{cases} \tau_{s1} = K_1 q + D_1 \dot{q} & \dot{q}_0 \dot{q} > 0, \\ \tau_{s2} = K_2 q + D_2 \dot{q} & \dot{q}_0 \dot{q} \leq 0. \end{cases} \tag{14}$$

where $\dot{q}_0$ is initial velocity. Equation (14) introduces a switching feedback policy. This kind of feedback might cause instability. From the linearized system (3) and linear feedback (14) the following system can be derived:

$$\begin{cases} \dot{x} = A_1 x & x_2(0)x_2 > 0, \\ \dot{x} = A_2 x & x_2(0)x_2 \leq 0, \\ A_1 = A + BF_1, A_2 = A + BF_2, \\ F_1 = B(K_1 x_1 + D_1 x_2), \\ F_2 = B(K_2 x_1 + D_2 x_2). \end{cases} \tag{15}$$

In the linearized system (15), A_1 and A_2 alone are stable based on condition (13) as far as $D > 0$ and $K - mgl > 0$. However, the closed loop system switches between A_1 and A_2 depending on the sign of the velocity. Furthermore, in practice the switching rate can occur quite often. For instant, when velocity is close to zero, noises in the velocity sensor or some disturbances affect the velocity feedback and switching could happen many times. In this case, the closed loop system stability is not guaranteed by the stability of A_1 and A_2 alone.

Equation (15) has the form of a polytopic system with a time varying parameter. It is not necessary to know when the switching (which depends on the velocity) occurs. The stability can be ensured by investigating if the system is quadratic or polyquadratic (parameter dependent Lyapunov) stable. A_1 and A_2 are the vertices of a polytopic system and using MATLAB commands quadstab (quadratic) and

TABLE II

FITTING OF MODEL (14) TO u^* WHILE THE $\dot{q_0} = \pm 0.9$

γ	K_1	D_1	K_2	D_2
0	110.0682	25.096	110.0682	25.096
100	115.088	10.36	76.86	18.67
200	112.76	10.077	67.50	13.844
300	111.34	9.99	62.70	10.066
400	110.51	9.94	61.25	9.222
500	109.81	9.919	60.40	8.77
600	109.17	9.915	59.85	8.554
700	108.76	9.902	58.118	5.865

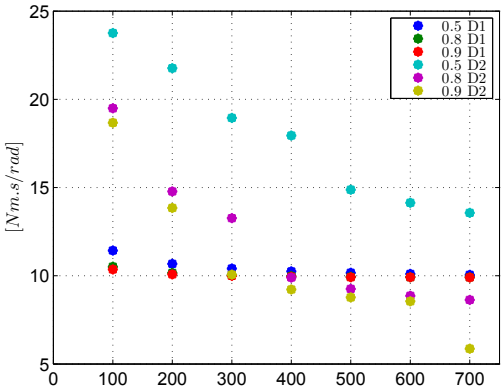

Fig. 8. Damping values D_1 and D_2 versus γ for different initial velocity, $\dot{q_0} = \pm\{0.5,\ 0.8,\ 0.9\}$.

pdlstab (polyquadratic) the stability can be evaluated. Either quadratic or polyquadratic stability are sufficient to ensure that (15) is stable no matter how fast the switching occurs.

For all γ in Table II from zero up to 600 quadratic stability holds. This means that the system is quadratically stable and that the feedback can be switched any time between the F_1 and F_2 at any rate and global stability is maintained. For $\gamma = 700$ the system is not quadratically stable however it may still be globally stable since quadratic stability is only a sufficient condition. Polyquadratic stability is less conservative. For all γ in Table II the system is polyquadratically stable. This analysis shows that the linearized system with the switching feedback is well behaved and stable.

The result of nonlinear regression fitting of model (14) for initial velocities of $\dot{q_0} = \pm 0.9$ are listed in Table II. The value of stiffnesses, K_1 and K_2 are plotted in Fig. 9 for all initial velocities $\dot{q_0} = \pm\{0.5,\ 0.8,\ 0.9\}$ for γ from zero to 700 with incremental of 100. Similar plot for damping, D_1 and D_2 are provided in Fig. 8. The ankle torque (14) with values extracted from nonlinear fitting for $\gamma = 700$ and $\dot{q_0} = 0.9$ is compared with its optimal control u^* in Fig. 10.

As discussed in end of subsection II-B introducing nonzero γ results in drop of the peak torque, x_{cop} and power. This results are valid for the approximate optimal compliance regulator (14) as it is evident from Fig. 10. Therefore, (14) maintains whole body balance in higher level of impacts than for optimal ankle compliance stabilizer ($\gamma = 0$).

Generally the levels of stiffness and damping reduce by increasing γ. It is evident that levels of damping are certainly bellow the damping of $\gamma = 0$ in Fig. 8. While D_1 shows little reduction, D_2 drops significantly by increasing the γ. Similar trend can be observed for the stiffness level. The first stiffness K_1 demonstrates a little variation and is a bit more

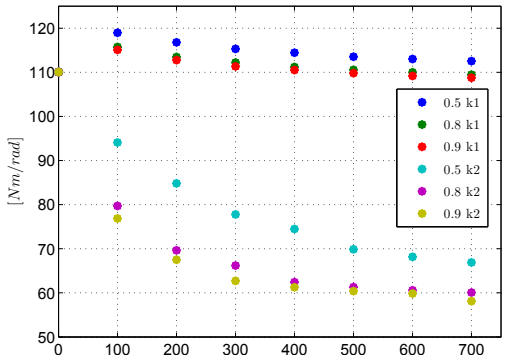

Fig. 9. Stiffness values K_1 and K_2 versus γ for different initial velocity $\dot{q_0} = \pm\{0.5,\ 0.8,\ 0.9\}$.

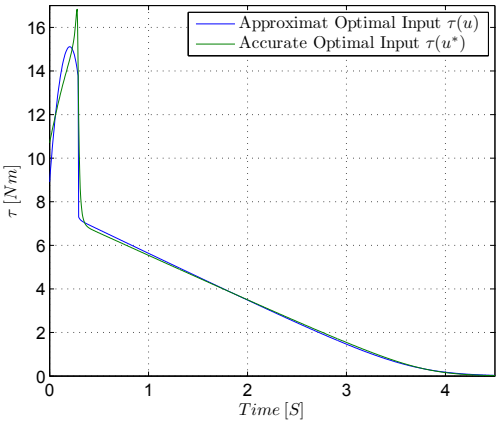

Fig. 10. Accurate (12) and approximate (14) optimal control input for impact equivalent to initial velocity of $\dot{q_0} = 0.9$ and $\gamma = 700$.

than K for $\gamma = 0$, while K_2 has substantial reduction by rising γ. Therefore when an impulsive impact occurs at zero position, lower damping coefficients give a reduction in the peak power. This in turn means that whole body stability of the humanoid can tolerate larger impacts.

In practice by measuring impact the first value of K_1 and D_1 will be applied on ankle pitch joint. When the humanoid reaches to zero velocity and maximum x_{com} deviation the ankle compliance of K_2 and D_2 will be set. The stability issues rising from switching is not concern since it is ensured by Polyquadratic stability method. For reducing the peak power, higher values of γ which means lower value of K_1 and D_1 should be used. Also the realization of the ankle variable compliance can done by admittance or impedance controllers [21]–[23].

Fig. 11 depicts the position of the simulated inverted pendulum model with initial velocity of $\dot{q_0} = 0.9[rad/s]$ while the approximate optimal compliance regulator (14) is applied with values in Fig. 8 and Fig. 9 for γ from zero to 700 by incremental of 100. This plot could confirm how close is the performance of the approximate optimal compliant regulator (14) to the optimal control (12).

Even that the peak torque can be reduced using J_2, inevitably there are sufficiently large impacts that require placing limits on the ankle torque (11) to prevent the x_{cop} leaving the support polygon. The limiting torque values are independent of the cost used (J_1 or J_2) and therefore the strategy dealing with this situation called *variable optimal*

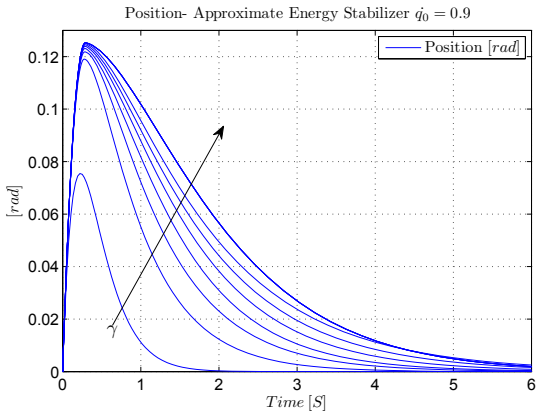

Fig. 11. Position, $q[rad]$ due to impact equivalent to initial velocity of 0.9 for γ from zero to 700 by incremental of 100 with approximate optimal compliance regulator (14).

compliance is the same as described in [14].

In addition to the provided simulation in the paper, the result of the proposed controller is evaluated by the full body COMAN simulator [24] which could demonstrate nice walking [25], pull up, push up, etc. tasks [26] in simulation compare to the practice.

III. Conclusion

The paper introduced a novel approximate optimal compliance regulation method which can be used to reduce the peak power of the ankle joint of a humanoid robot during balancing regulation against external disturbances. The ability of the method to keep balance of humanoid for a wide range of impacts was illustrated. The stability of the approximate compliance controller was also evaluated by parameter dependent Lyapunov stability from practical point of view.

Acknowledgment

This work is supported by the ICT-248311-AMARSI and the FP7-ICT-2013-10 WALK-MAN European Commission projects.

References

[1] D. A. Winter, "Human balance and posture control during standing and walking," *Gait & Posture*, vol. 3, no. 4, pp. 193–214, 1995.

[2] A. Kuo, "An optimal control model for analyzing human postural balance," *IEEE Transactions on Biomedical Engineering*, vol. 42, no. 1, pp. 87–101, 1995.

[3] P. Gatev, S. Thomas, T. Kepple, and M. Hallett, "Feedforward ankle strategy of balance during quiet stance in adults," *The Journal of Physiology*, vol. 514, no. 3, pp. 915–928, 1999.

[4] P. G. Morasso and V. Sanguineti, "Ankle muscle stiffness alone cannot stabilize balance during quiet standing," *Journal of Neurophysiology*, vol. 88, no. 4, pp. 2157–2162, 2002.

[5] B. Stephens and C. Atkeson, "Dynamic balance force control for compliant humanoid robots," in *IEEE/RSJ International Conference on Intelligent Robots and Systems*. IEEE, 2010, pp. 1248–1255.

[6] S.-H. Hyon, "Compliant terrain adaptation for biped humanoids without measuring ground surface and contact forces," *IEEE Transactions on Robotics*, vol. 25, no. 1, pp. 171–178, 2009.

[7] Z. Li, B. Vanderborght, N. G. Tsagarakis, L. Colasanto, and D. G. Caldwell, "Stabilization for the cmpliant humanoid robot coman exploiting intrinsic and controlled compliance," in *Robotics and Automation (ICRA), 2012 IEEE International Conference on*. IEEE, 2012, pp. 2000–2006.

[8] Y. Huang and Q. Wang, "Gait selection and transition of passivity-based bipeds with adaptable ankle stiffness," *Int J Adv Robotic Sy*, vol. 9, no. 99, 2012.

[9] R. Ghorbani and Q. Wu, "On improving bipedal walking energetics through adjusting the stiffness of elastic elements at the ankle joint," *International Journal of Humanoid Robotics*, vol. 6, no. 01, pp. 23–48, 2009.

[10] M.-S. KIM and H. O. JUN, "Posture control of a humanoid robot with a compliant ankle joint," *International Journal of Humanoid Robotics*, vol. 7, no. 01, pp. 5–29, 2010.

[11] M. Garabini, A. Passaglia, F. Belo, P. Salaris, and A. Bicchi, "Optimality principles in variable stiffness control: The vsa hammer," in *International Conference on Intelligent Robots and Systems*. IEEE/RSJ, 2011, pp. 3770–3775.

[12] S. Haddadin, M. Weis, S. Wolf, and A. Albu-Schäffer, "Optimal control for maximizing link velocity of robotic variable stiffness joints," in *IFAC World Congress*, 2011.

[13] N. G. Tsagarakis, I. Sardellitti, and D. G. Caldwell, "A new variable stiffness actuator (compact-vsa): Design and modelling," in *Intelligent Robots and Systems (IROS), 2011 IEEE/RSJ International Conference on*. IEEE, 2011, pp. 378–383.

[14] M. Mosadeghzad, Z. Li, N. G. Tsagarakis, G. A. Medrano-Cerda, H. Dallali, and D. G. Caldwell, "Optimal ankle compliance regulation for humanoid balancing control," in *IEEE/RSJ International Conference on Intelligent Robots and Systems (IROS)*. IEEE, 2013, pp. 4118–4123.

[15] N. Tsagarakis, S. Morfey, G. Medrano-Cerda, Z. Li, and D. G. Caldwell, "Compliant humanoid coman: Optimal joint stiffness tuning for modal frequency control," in *IEEE International Conference on Robotics and Automation*, Karlsruhe, Germany, 2013.

[16] N. G. Tsagarakis, Z. Li, J. Saglia, and D. G. Caldwell, "The design of the lower body of the compliant humanoid robot ccub," in *International Conference on Robotics and Automation*. IEEE, 2011, pp. 2035–2040.

[17] N. G. Tsagarakis, F. Becchi, L. Righetti, A. Ijspeert, and D. G. Caldwell, "Lower body realization of the baby humanoid-icub," in *Intelligent Robots and Systems, 2007. IROS 2007. IEEE/RSJ International Conference on*. IEEE, 2007, pp. 3616–3622.

[18] S. Kajita, K. Yokoi, M. Saigo, and K. Tanie, "Balancing a humanoid robot using backdrive concerned torque control and direct angular momentum feedback," in *IEEE International Conference on Robotics and Automation*, vol. 4. IEEE, 2001, pp. 3376–3382.

[19] D. E. Kirk, *Optimal control theory: an introduction*. Dover Publications, 2004.

[20] J.-J. E. Slotine, W. Li, *et al.*, *Applied nonlinear control*. Prentice hall New Jersey, 1991, vol. 1, no. 1.

[21] Z. Li, N. Tsagarakis, and D. G. Caldwell, "A passivity based admittance control for stabilizing the compliant humanoid coman," in *IEEE-RAS International Conference on Humanoid Robots*. IEEE, 2012, pp. 44–49.

[22] M. Mosadeghzad, G. Medrano-Cerda, J. Saglia, N. G. Tsagarakis, and D. Caldwell, "Comparison of various active impedance control approaches, modeling, implementation, passivity, stability and trade-offs," in *International Conference on Advanced Intelligent Mechatronics*. IEEE/ASME, 2012, pp. 342–348.

[23] M. Mosadeghzad, G. Medrano Cerda, N. G. Tsagarakis, and D. G. Caldwell, "Impedance control with inner pi torque loop: Effects of load dynamics, disturbance attenuation and impedance emulation," in *Robotics and Biomimetics, International Conference (IEEE-ROBIO)*, 2013.

[24] H. Dallali, M. Mosadeghzad, G. Medrano-Cerda, N. Docquier, P. Kormushev, N. Tsagarakis, Z. Li, and D. Caldwel, "Development of a dynamic simulator for a compliant humanoid robot based on a symbolic multibody approach," in *International Conference on Mechatronics*. IEEE, 2013.

[25] Z. Li, N. G. Tsagarakis, and D. G. Caldwell, "Walking pattern generation for a humanoid robot with compliant joints," *Autonomous Robots*, pp. 1–14, 2013.

[26] H. Dallali, M. Mosadeghzad, G. Medrano Cerda, V. Loc, N. G. Tsagarakis, M. Gesino, and D. G. Caldwell, "Designing a high performance humanoid robot based on dynamic simulation," in *UKSim-AMSS 7th European Modelling Symposium on Mathematical Modelling and Computer Simulation (EMS), Manchester,UK.*, 2013.